pillary column with a 0.32-mm i.d. and a 0.25-μm coating. The column temperature was isothermal at 210 °C with detection by FID at 280 °C. Temperature at the injector port was 230 °C. Retention times were as follows: methyl linoleate, 8.04 min; methyl oleate, methyl vaccenate, and methyl petroselenate, 7.93 min; 9,12(*E*,*E*)-methyl octadecadienate, 8.05 min; 9(*Z*)-methyl 12,13-epoxyoctadecenoate, 20.72 min; 12(*Z*)-methyl 9,10-epoxyoctadecenoate, 21.08 min; 9(*E*)-methyl 12,13-epoxyoctadecenoate, 19.27 min; 12(*Z*)-methyl 9,10-epoxyoctadecenoate, 19.45 min; 6,7-methyl epoxystearate, 19.80 min; methyl 9,10-epoxystearate, 20.53 min; methyl 11,12-epoxystearate, 20.90 min. Steroids were analyzed on a 30-m SPB-1 (nonpolar) bonded phase capillary column with a 0.32-mm i.d. and a 0.25-μm coating. The column temperature was isothermal at 260 °C. Retention times were as follows: cholesterol, 17.5 min; 5α,6α-epoxycholesterol, 22.5 min; 5β,6β-epoxycholesterol, 23.4 min; 25-hydroxycholesterol, 26.4 min; stigmasterol, 22.7 min; 22,23-epoxystigmasterol, 26.2 min; fucosterol, 25.3 min; 24,28-epoxyfucosterol, 33.4 min. Desmosterol and its reaction products were analyzed as 3β-trimethylsilyl ethers after derivatization with chlorotrimethylsilane and hexamethyldisilazane: desmosterol, 21.8 min; 5β,6β-epoxydesmosterol, 28.6 min; 5α,6α-epoxydesmosterol, 30.5 min; 24,25-epoxydesmosterol, 29.1 min. 25-Hydroxycholesterol was also identified by GC-MS and compared to an authentic sample (Research Plus). The retention time was 26.4 min. MS: *m/z* 402 (24), 384 (100), 369 (47), 367 (13), 351 (36), 300 (28), 299 (33), 273 (38), 271 (69), and lower *m/z* steroidal clusters.

Acknowledgment. Support for the research by the National Science Foundation (Grant CHE-87-06310) is gratefully acknowledged. The NSF and NIH provided funds for the purchase of the high-resolution FABMS-GC.

Quantification of Singlet Oxygen Generated by Thermolysis of 3,3′-(1,4-Naphthylidene)dipropionate. Monomol and Dimol Photoemission and the Effects of 1,4-Diazabicyclo[2.2.2]octane

Paolo Di Mascio and Helmut Sies*

Contribution from the Institut für Physiologische Chemie I, Universität Düsseldorf, Moorenstr. 5, D-4000 Düsseldorf, FRG. *Received March 25, 1988*

Abstract: Singlet oxygen arising from the thermal decomposition of the water-soluble endoperoxide of 3,3′-(1,4-naphthylidene)dipropionate ($NDPO_2$) or from hypochlorite/H_2O_2 was detected. Direct measurements of light emission due to the chemiluminescent transition of O_2 ($^1\Delta_g$) to the triplet ground state was monitored (a) by monomol emission in the near-infrared (1270 nm) with a liquid nitrogen cooled germanium diode and (b) by dimol emission in the visible spectral region (634 and 703 nm) with a red-sensitive photomultiplier and photon counting. Chemical trapping of $^1O_2$ generated by $NDPO_2$ or by hypochlorite/H_2O_2 was used for quantification with the anthracene-9,10-diyldiethyl disulfate (EAS), yielding the endoperoxide ($EASO_2$) as the specific oxidation product. The β value for $EASO_2$ was calculated to be 7.7×10^{-3} M and 8×10^{-3} M when $^1O_2$ was generated by $NDPO_2$ or hypochlorite/H_2O_2, respectively. Due to the enhancement of the lifetime of $^1O_2$, the β values were lower in D_2O. The yields of $^1O_2$ were measured, showing that one-half of the O_2 liberated by thermolysis of $NDPO_2$ was in the singlet state, whereas the yield for hypochlorite/H_2O_2 was near unity. The addition of 1,4-diazabicyclo[2.2.2]octane (DABCO) increased dimol emission with a concomitant decrease of monomol light emission, but left the yield of $EASO_2$ unchanged. Similar results were obtained with hypochlorite/H_2O_2. A calibration of the photoemission was performed, based on the $^1O_2$ yield of $NDPO_2$ thermodissociation.

1. Introduction

Several methods have been described for the generation of singlet molecular oxygen ($^1O_2$), e.g. photosensitization, chemical oxidants, and microwave discharge. Chemical sources of $^1O_2$ include aromatic endoperoxides that liberate $^1O_2$ by thermolysis.[1-4] Such compounds can be individually designed to exhibit desired solubility characteristics and thermodissociation temperature. Aromatic endoperoxides such as alkyl- and aryl-substituted naphthalenes decompose thermally in solution into the parent hydrocarbon and molecular oxygen.[4-7] We studied the thermal decomposition of the water-soluble disodium salt 3,3′-(1,4-naphthylidene)dipropionate ($NDPO_2$),[4] as shown in reaction 1.

We describe the quantification of $^1O_2$ generated by the thermal decomposition of $NDPO_2$ using a chemical trap, the water-soluble sodium salt of anthracene-9,10-diyldiethyl disulfate (EAS), and

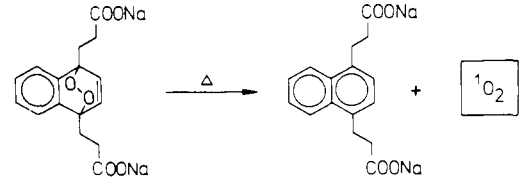

Endoperoxide of Disodium 3,3′-(1,4-Naphthylidene) Dipropionate ($NDPO_2$)

Disodium 3,3′-(1,4-Naphthylidene) Dipropionate (NDP)

(1)

the employment of sodium azide as $^1O_2$ quencher as well as the detection of monomol (reaction 2) and dimol (reaction 3) emission.

$$O_2(^1\Delta_g) \rightarrow O_2(^3\Sigma^-_g) + h\nu \quad (1270\ \text{nm}) \qquad (2)$$

$$2O_2(^1\Delta_g) \rightarrow 2O_2(^3\Sigma^-_g) + h\nu \quad (634, 703\ \text{nm}) \qquad (3)$$

Further, we report new observations on the effect of DABCO on monomol and dimol emission, and we show the calibration of the photoemission signals. The effects are compared to those obtained with hypochlorite/H_2O_2.

2. Experimental Section

2.1. Reagents. Reagents were purchased from the following sources: 1,4-dimethylnaphthalene, benzoyl peroxide, azodiisobutyronitrile, *N*-

(1) Foote, C. S.; Shook, F. C.; Abakerli, R. A. *Methods Enzymol.* **1984**, *105*, 36-47.
(2) Wasserman, H. H.; Scheffer, J. R. *J. Am. Chem. Soc.* **1967**, *89*, 3073.
(3) Turro, N. J.; Chow, M. F.; Rigaudy, J. *J. Am. Chem. Soc.* **1981**, *103*, 7218-7224.
(4) Aubry, J. M. *J. Am. Chem. Soc.* **1985**, *107*, 5844-5849.
(5) Saito, I.; Matsuura, T.; Inoue, K. *J. Am. Chem. Soc.* **1983**, *105*, 3200-3206.
(6) Chou, P. T.; Frei, H. *Chem. Phys. Lett.* **1985**, *122*, 87-92.
(7) Saito, I.; Nagata, R.; Nakagawa, H.; Momiyama, H.; Matsuura, T.; Inoue, K. *Free Radical Res. Commun.* **1986**, *2*, 327-336.

0002-7863/89/1511-2909$01.50/0

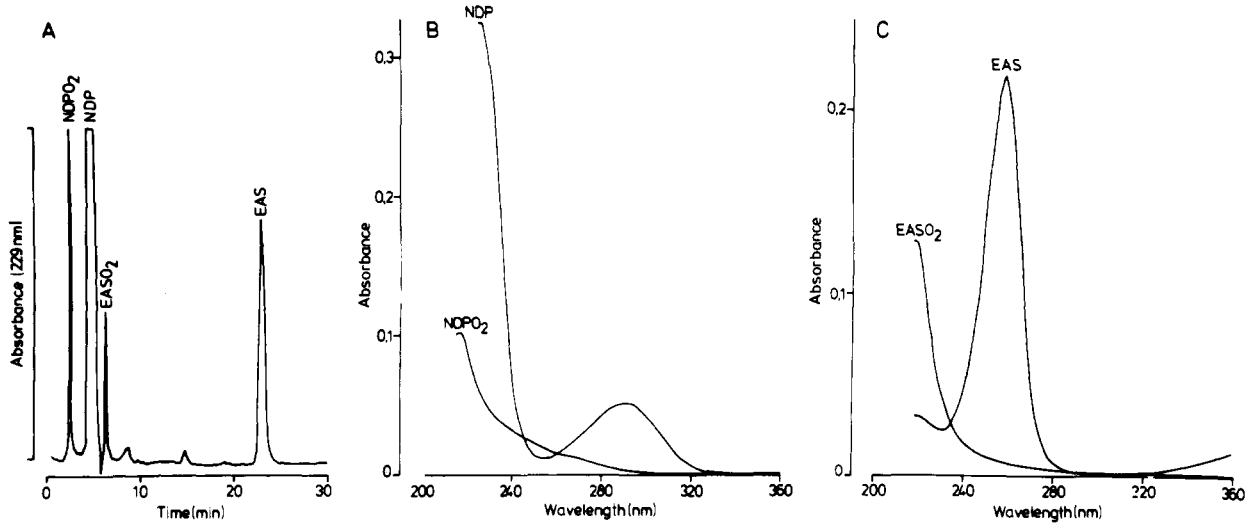

Figure 1. Chemical detection of singlet oxygen by formation of the endoperoxide of anthracene-9,10-diyldiethyl disulfate according to reaction 4: (A) chromatogram; (B) absorbance spectra of NDP and $NDPO_2$; (C) EAS and $EASO_2$ after separation by HPLC and detection with a multichannel photodetector. EAS (2 mM) was exposed to $^1O_2$, generated by the endoperoxide $NDPO_2$ (6 mM), for 20 min. Conditions: 37 °C, pH 7.4, 50 mM phosphate buffer.

bromosuccinimide, and sodium hypochlorite from the Aldrich Chemical Co. (Milwaukee, WI) and molybdic acid, sodium salt from the Sigma Chemical Co. (Munich, FRG). Malonic acid diethyl ester and nitrobenzene were distilled. 1,4-Dimethylnaphthalene and malonic acid diethyl ester were analyzed by their ^1H NMR and infrared spectra. Anthracene-9,10-diyldiethyl disulfate is a generous gift from Prof. A. P. Schaap (Department of Chemistry, Wayne State University, Detroit, MI); other chemicals were from Merck (Darmstadt, FRG).

2.2. Syntheses. 1,4-Naphthalenedipropionic acid, sodium salt (NDP) was prepared by a modification of the method described by Saint-Jean and Cannone.[8] 1,4-Bis(bromomethyl)naphthalene was prepared by bromination of 1,4-dimethylnaphthalene. In a dry 2-L flask a solution of 70 g (0.45 mol) of purified 1,4-dimethylnaphthalene was placed in 800 mL of reagent grade carbon tetrachloride. Benzoyl peroxide (2 g), azodiisobutyronitrile (2 g), and 175 g (0.1 mol) of *N*-bromosuccinimide were powdered, mixed well, and added to the flask. The solution was refluxed and irradiated with an ultraviolet source for 1 h and then allowed to sit overnight at ambient temperature. The solvent was removed in vacuo; the residue was then warmed in chloroform on a steam cone and filtered hot. The crude succinimide residue was then digested several times with hot chloroform to remove all remaining product. Repeated recrystallization of the product was performed from benzene. Diethyl α,α'-dicarbethoxy-1,4-naphthalenedipropionate was prepared by malonic synthesis according Marvel and Wilson.[9] The saponification and decarboxylation of diethyl α,α'-dicarbethoxy-1,4-naphthalenedipropionate was by the procedure of Lock and Walter.[10] 1,4-Naphthalenedipropionic acid, disodium salt (NDP) was prepared by neutralization of the 1,4-naphthalenedipropionic acid by sodium methylate in methanol and precipitation with ether. The product was filtered through a column (35 × 210 mm) of activated alumina.

Endoperoxide of the disodium salt of 3,3'-(1,4-naphthylidene)dipropionate ($NDPO_2$) was prepared by the H_2O_2/Na_2Mo_4 method described by Aubry.[4] The products were identified by ^1H NMR and IR spectroscopy.

2.3. Generation of Singlet Oxygen by $NDPO_2$ or by Hypochlorite/H_2O_2. Singlet oxygen generated chemically was observed upon the thermodissociation of the endoperoxide of 3,3'-(1,4-naphthylidene)dipropionate ($NDPO_2$) or the hypochlorite/H_2O_2 system. $NDPO_2$ dissociates, yielding the 3,3'-(1,4-naphthylidene)dipropionate (NDP) and molecular oxygen (reaction 1). At 37 °C, 3 mL of 50 mM, pH 7.4 phosphate buffer in H_2O or D_2O was placed in a thermostated glass cuvette of (35 mm × 6 mm × 55 mm). D_2O was 90% of the solution with $NDPO_2$ alone; there was 80% D_2O when $NDPO_2$ was used with EAS or NaN_3 and 38% D_2O in the hypochlorite/H_2O_2 system. The reaction was started by adding 25 μL of $NDPO_2$ (0.6 M) at 2 °C to the solution under constant stirring with a small magnetic bar. Thermal equilibrium was achieved within 12–15 s. $NDPO_2$ concentration was determined spectrophotometrically with an LKB spectrophotometer (Model Ultrospec 4050). For hypochlorite/H_2O_2, NaOCl (0.27 M) was infused at a rate of 20 μL min^{-1} during 5 min (total NaOCl infused was 9 mM) into 3 mL of 21 mL H_2O_2 at 37 °C. Sodium hypochlorite and H_2O_2 were analyzed iodometrically.

2.4. Singlet Molecular Oxygen Monomol Emission (1270 nm). Infrared emission of $^1O_2$ was measured with a liquid nitrogen cooled germanium photodiode detector (Model EO-817L, North Coast Scientific Co., Santa Rosa, CA) sensitive in the spectral region from 800 nm to 1800 nm with a detector area of 0.25 cm^2 and a sapphire window. The Ge-diode signal was processed with a Lock-in amplifier (Model 5205, EG&G, Brookdeal Electronics Princeton Applied Research). An oscilloscope (Model 1222A, Hewlett-Packard Co.) was simultaneously used with the amplifier, the chopper, and the germanium-photodiode detector. The optical chopper (Model OC 400, Photon Technology Int.) was used with a frequency of 30 s^{-1}. Measurements were carried out in a cuvette with mirrored walls (35 mm × 6 mm × 55 mm).

2.5. Singlet Molecular Oxygen Dimol Emission (634 and 703 nm). Low-level chemiluminescence was measured with a single photon counting-system, as described in detail elsewhere,[11] equipped with a red-sensitive photomultiplier (EMI 9658 AM), cooled to −25 °C by a thermoelectric cooler. Selective light emission at 634, 668, and 703 nm was obtained by interference filters (Jenaer Glaswerk Schott, Mainz, FRG) which were placed between the cuvette and the photomultiplier tube. The light transmitted through these filters was expressed as the percentage of the total light detected by the photomultiplier tube after correcting for the peak transmission and the spectral sensitivity of each filter.

2.6. Chemical Detection of Singlet Molecular Oxygen. The generation of $^1O_2$ by $NDPO_2$ was monitored by chemical trapping with the water-soluble disodium salt of anthracene-9,10-diyldiethyl disulfate (EAS) (reaction 4).[16-18]

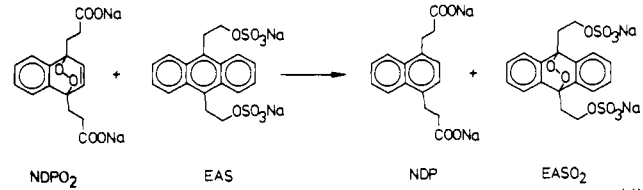

(4)

(8) Saint-Jean, R.; Cannone, P. *Bull. Soc. Chim. Fr.* **1971**, 3330–3335.
(9) Marvel, C. S.; Wilson, B. D. *J. Org. Chem.* **1958**, *23*, 1483–1488.
(10) Lock, G.; Walter, E. *Ber. Ges.* **1942**, *75B*, 1158–1163.
(11) Cadenas, E.; Sies, H. *Methods Enzymol.* **1984**, *105*, 221–231.
(12) Merkel, P. B.; Kearns, D. R. *J. Am. Chem. Soc.* **1972**, *94*, 7244–7253.
(13) Aubry, J. M.; Rigaudy, J.; Cuong, N. K. *Photochem. Photobiol.* **1980**, *33*, 155–158.
(14) Rodgers, M. A. J.; Snowden, P. T. *J. Am. Chem. Soc.* **1982**, *104*, 5541–5543.
(15) Rodgers, M. A. J. *J. Am. Chem. Soc.* **1983**, *105*, 6201–6205.
(16) Botsivali, M.; Evans, D. F. *J. Chem. Soc., Chem. Commun.* **1979**, 1114–1116.
(17) Evans, D. F.; Upton, M. W. *J. Chem. Soc., Dalton Trans.* **1985**, 1141–1145.

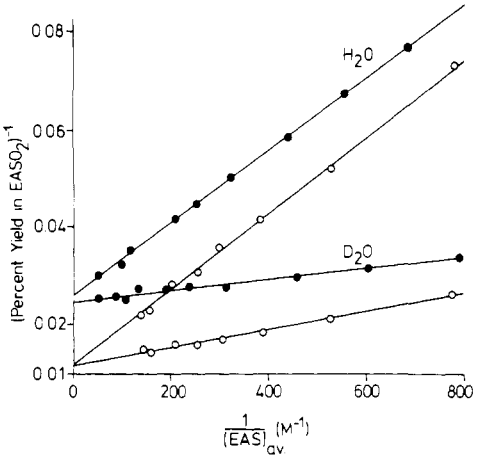

Figure 2. Plot of (percent yield in $EASO_2$)$^{-1}$ against $(EAS_{av})^{-1}$ of the reaction of $NDPO_2$ (6 mM) (●) and hypochlorite/H_2O_2 (○). Conditions: $NDPO_2$ was incubated at 37 °C during 2 h, pH 7.4, 50 mM phosphate buffer. NaOCl (0.27 M) was infused at a rate of 20 μL min^{-1} during 15 min (total NaOCl infused 0.114 M) into 900 μL of 30 mM H_2O_2. The reactions were carried out under constant stirring in the presence of different concentrations of EAS in H_2O or D_2O. As indicated in the Experimental Section, the D_2O content was 80% with $NDPO_2$ and 38% with hypochlorite/H_2O_2. The plot is according to eq 4 in ref 17.

The endoperoxide $EASO_2$ as the reaction product characteristic of $^1O_2$ was separated from EAS, NDP, and $NDPO_2$ by isocratic reverse-phase HPLC (Figure 1A) performed on a C_{18} column using a mobile phase consisting of 70% aqueous ammonium acetate (100 mM) and 30% methanol. The flow rate was 2.0 mL/min and the detection was at 229 nm. The characterization of the reaction products was performed by UV spectroscopy after HPLC separation (Figure 2B,C).

2.7. Chemical Quantification of Singlet Molecular Oxygen. $^1O_2$ was detected by the oxidation of the chemical trap (EAS) to the $^1O_2$ endoperoxide product ($EASO_2$). The reactivity of EAS toward $^1O_2$ was expressed by its β value, the concentration at which 50% of the available $^1O_2$ is trapped.[19] The β value of EAS was determined directly in water and deuterium oxide with $NDPO_2$ and the reaction of hypochlorite with H_2O_2 from a double-reciprocal plot of the efficiency expressed as percent yield in $EASO_2$ vs the average concentration of EAS, $[EAS]_{av}$.[16,17] $[EAS]_{av}$ is taken as the mean of the initial and final concentrations of EAS, and it was obtained from the absorbance at 396 nm. The error involved due to changes in the EAS during the reaction was minimized by limiting the oxidation of EAS to 20% or less. The extinction coefficient of EAS at 396 nm was determined with a Model 25 spectrophotometer (Beckman Instruments, Palo Alto, CA). The value ($\epsilon = (9.2 \pm 0.4) \times 10^3$ M^{-1} cm^{-1}) is a mean of quadruplicate measurements of five different stock solutions prepared by weighing.

3. Results

3.1. Determination of the Yield of $^1O_2$ Generated by $NDPO_2$ or Hypochlorite/H_2O_2 Using the β Value of the Endoperoxide $EASO_2$. From experiments such as that shown in Figure 1A, a double-reciprocal plot of percent yield in $EASO_2$ against $[EAS]_{av}$ was obtained for the reaction of $NDPO_2$ or hypochlorite/H_2O_2 (Figure 2). The β value, corresponding to the EAS concentration required to obtain a yield of $EASO_2$ of 50%, was found to be 7.7 $\times 10^{-3}$ M in water and 1.1 $\times 10^{-3}$ M in 80% D_2O for $NDPO_2$ and 8 $\times 10^{-3}$ M in water and 3 $\times 10^{-3}$ M in 38% D_2O for hypochlorite/H_2O_2. The ratio of the two β values should represent the ratio of the lifetimes of $^1O_2$ in H_2O and in D_2O. The 7-fold diffrerence when $^1O_2$ is generated by $NDPO_2$ in D_2O vs H_2O is attributed to the longer lifetime of $^1O_2$ in 80% D_2O. The lower ratio obtained with the hypochlorite/H_2O_2 system may be due to the lower percentage of D_2O in the solution. The ratio of the lifetimes in H_2O/D_2O was reported to be in the range of 10–14.[12-15] In mixtures with H_2O, the lifetime of $^1O_2$ is linearly related to the percentage of D_2O,[15] and we extrapolate the ratio of β values to 8 for 100% D_2O.

Table I. Relative Light Emission Produced at 634, 668, and 703 nm by Thermodissociation of $NDPO_2$[a]

	relative % light emission[b]			
open	634 nm	668 nm	703 nm	634 nm + 703 nm
100	22 ± 2.5 (6)	0.15 ± 0.10 (3)	31.1 ± 1.5 (5)	53.1

[a] Conditions as described in Figure 5, with 30 mM $NDPO_2$. [b] The relative amount of light passing each interference filter (calculated as a percentage) compared to the total light emitted over a bandwidth of approximately 400–750 nm. Data were corrected for the maximum transmission characteristics of each filter within the filter passband, and data are means ± SEM (n) and are corrected for spectral sensitivity of the photomultiplier tube.

When $^1O_2$ is produced in the presence of EAS, it may follow three main pathways:[16,17] quenching by solvent (reaction 5), quenching by EAS (reaction 6), or reaction with EAS (reaction 7).

$$^1O_2 + S \rightarrow {}^3O_2 + S \quad (5)$$

$$^1O_2 + EAS \rightarrow {}^3O_2 + EAS \quad (6)$$

$$^1O_2 + EAS \rightarrow EASO_2 \quad (7)$$

The yield in $EASO_2$ is calculated from eq 4 in ref 17 by plotting data from experiments such as that shown in Figure 1A for different concentrations of EAS. The intercept in Figure 2 indicates a yield of 41% $^1O_2$ for $NDPO_2$ and of 87% for hypochlorite/H_2O_2. Information on the contribution of reaction 6 can be obtained by examining the yield of $EASO_2$ at the concentration of EAS at the β value. The fraction of oxygen present in the singlet state can be calculated from equation 5 in ref 17. The percentage of the yield in $^1O_2$ thus calculated is 51 ± 2% (n = 3) for $NDPO_2$ and 93 ± 2% (n = 3) for hypochlorite/H_2O_2.

It is noteworthy that, from the hypochlorite/H_2O_2 data reported in ref 17 and 20, a 30% and 10% difference, respectively, in the $^1O_2$ yield obtained from evaluation according to eq 4 and 5 in ref 17 can also be calculated. Thus, we conclude that there is a slight activity in physical quenching of $^1O_2$ by EAS.

3.2. Singlet Oxygen Monomol and Dimol Emission. The monomol $^1O_2$ light emission is directly proportional to the concentration of $NDPO_2$ (Figure 3A). The dimol light emission is proportional to the square of the $NDPO_2$ concentration (Figure 3B). In similar work using hypochlorite/H_2O_2, Deneke and Krinsky[21] found a more complex dependence on $[^1O_2]^2$ with two slopes and a breakpoint at 0.5 M^2 of [NaOCl]^2. The light emission by $NDPO_2$ at 634 and 703 nm is 53.1% of the total light emitted, whereas at 668 nm it is only 0.15% (Table I). This pattern was considered characteristic and diagnostic for $^1O_2$ dimol emission.[22] It also indicates that light is emitted in the visible range of the spectrum; this visible photoemission is being further investigated (Di Mascio, P.; Sies, H., unpublished).

The replacement of H_2O by 90% D_2O led to a 20-fold increase in the monomol light emission (Figure 3A) and only a 3-fold increase in the dimol band at 703 nm (Figure 3B). The loss of the Ge-diode signal with increased concentrations of the chemical trap EAS or the quencher sodium azide is shown in Figure 4. Figure 4A,C shows the time course of the light emission before and after the addition of EAS or NaN_3, and Figure 4B,D shows the concentration dependence. The half-maximal concentrations were 0.18 mM and 14 μM for EAS and azide, respectively.

3.3. Effect of DABCO. DABCO has been described to stimulate $^1O_2$ dimol emission.[21,23,24] Figure 5A shows that DABCO has no effect on the thermodissociation kinetics. The monomol light emission (Figure 5B) and the dimol light emission at 703 nm (Figure 5C) exhibit opposite behavior. DABCO enhances

(18) Lindig, B. A.; Rodgers, M. A. J.; Schaap, A. P. *J. Am. Chem. Soc.* **1980**, *102*, 5590–5593.
(19) Foote, C. S. In *Free Radicals in Biology*; Pryor, W. A., Eds.; Academic Press: New York, 1976; pp 85–133.
(20) McCall, D. Ph.D. Thesis, Wayne State University, 1984.
(21) Deneke, C. F.; Krinsky, N. I. *Photochem. Photobiol.* **1977**, *25*, 299–304.
(22) Khan, A. U.; Kasha, M. *J. Am. Chem. Soc.* **1970**, *92*, 3293–3300.
(23) Deneke, C. F.; Krinsky, N. I. *J. Am. Chem. Soc.* **1976**, *98*, 3041–3042.
(24) Lengfelder, E.; Cadenas, E.; Sies, H. *FEBS Lett.* **1983**, *164*, 366–370.

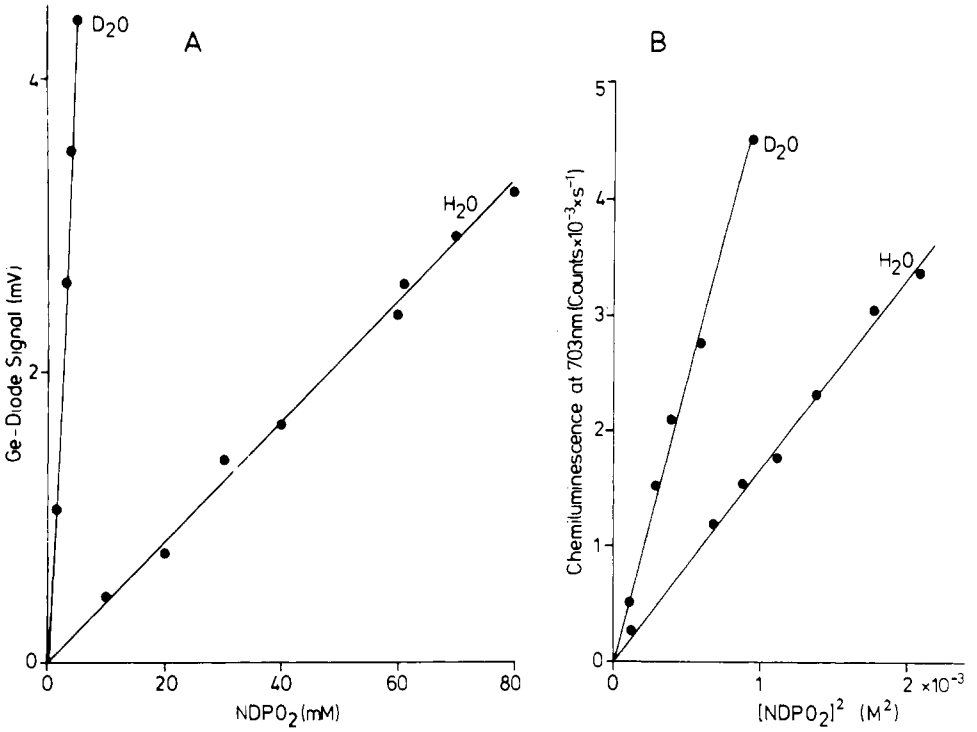

Figure 3. Monomol and dimol light emission as a function of $NDPO_2$ concentration: (A) proportional to the $NDPO_2$ concentration, detected by a germanium diode, and (B) proportional to the square of the $NDPO_2$ concentration, detected by a photomultiplier at 703 nm. Conditions: 37 °C, pH 7.4, in H_2O or 90% D_2O phosphate buffer (50 mM).

Table II. Effect of NaN_3 on $EASO_2$ Formation by Different $^1O_2$-Generating Systems[a]

	relative % $EASO_2$[b]	
NaN_3, mM	$NDPO_2$ (thermodissociation)	OCl^-/H_2O_2
in H_2O		
	100 ± 11 (12)	100 ± 4 (6)
0.4	46 ± 6 (3)	51 ± 5 (3)
in D_2O (38%)		
	143 ± 10 (3)	155 ± 9 (3)
0.4	47 ± 5 (3)	62 ± 8 (3)

[a] Conditions: $NDPO_2$ (5 mM), EAS (10 mM or 3 mM) in phosphate buffer 50 mM, pH 7.4. The solutions were incubated at 37 °C during 2 h. The reaction of NaOCl with H_2O_2 was as described in Figure 2, EAS (3 mM). [b] The relative amount of $EASO_2$ as determined by HPLC (compare Figure 1) is presented as percent of control. Data are means values ±SEM from (n) different experiments.

the dimol emission and decreases the monomol signal in a concentration-dependent manner when $^1O_2$ is generated by $NDPO_2$ (Figure 6A) or by hypochlorite/H_2O_2 (Figure 6B). No change in the yield of $EASO_2$ was observed in the presence of DABCO up to 150 mM when $^1O_2$ was generated by $NDPO_2$ or hypochlorite/H_2O_2 (data not shown).

Replacing H_2O by 38% D_2O led to an increase in $EASO_2$ by 50% both for $NDPO_2$ and the hypochlorite/H_2O_2 system (Table II). Sodium azide (0.4 mM) led to a decrease by one-half of the amount of $EASO_2$ both in H_2O and D_2O.

3.4. Stability of EAS and Selectivity for $EASO_2$ Formation with Other Oxidative Species. Table III shows that EAS did not react to yield $EASO_2$ with oxidants such as H_2O_2, superoxide anion, and triplet oxygen. Ozone,[25] hypochlorite, and hydroxyl radical show some reaction, but it is important to note that the products did not include $EASO_2$. On the basis of this information, $EASO_2$ can be considered as a specific singlet oxygen product.

4. Discussion

4.1. EAS as Singlet Oxygen Trap: Specificity and Efficiency (β Value). Singlet oxygen generation by the thermal decompo-

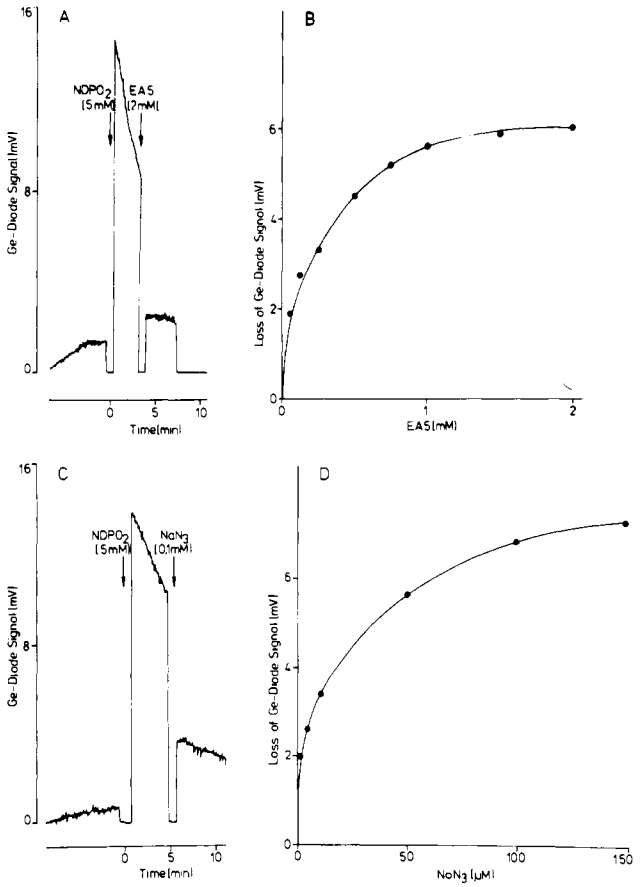

Figure 4. Effect of EAS and NaN_3 on the monomol light emission of singlet oxygen generated by $NDPO_2$: (A) effect of 2 mM EAS on the time course of light emission, (B) dependence of loss of germanium-diode signal on EAS concentration, (C) effect of 0.1 mM NaN_3, and (D) concentration dependence. Conditions: 37 °C, pH 7.4, in 80% D_2O phosphate buffer (50 mM).

(25) Wefers, H.; Schulte-Frohlinde, D.; Sies, H. *FEBS Lett.* **1987**, *211*, 49–52.

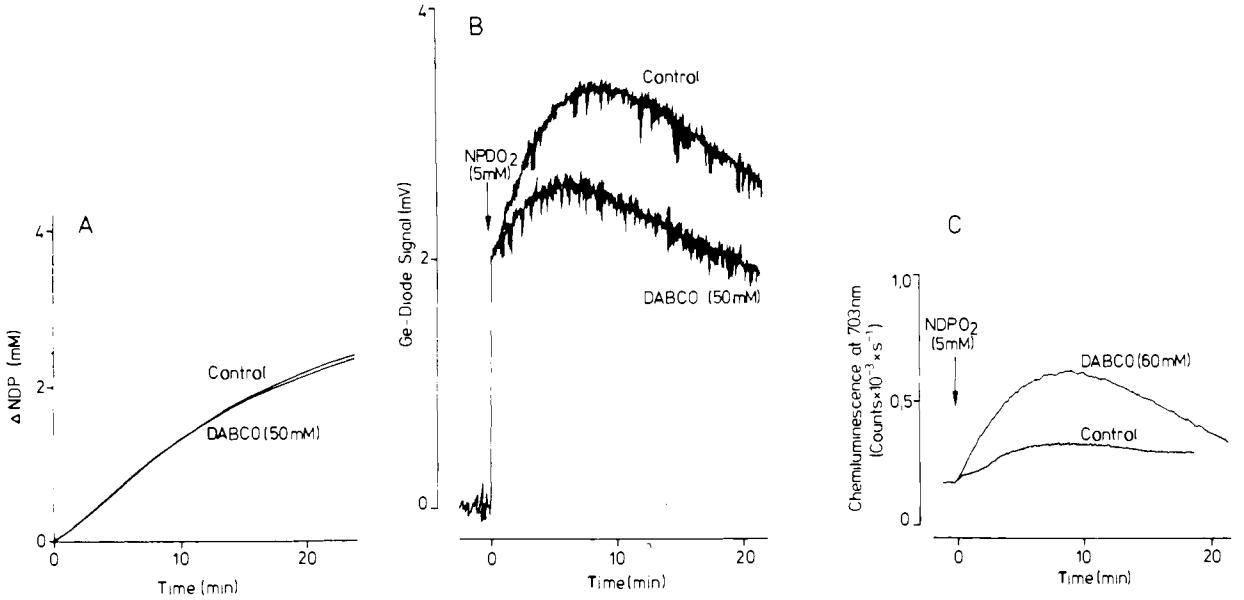

Figure 5. Effect of DABCO on the thermodissociation of $NDPO_2$, and on the monomol and the dimol light emission: (A) effect of DABCO on the time course of the thermodissociation of $NDPO_2$ (5 mM), (B) on the monomol light emission, and (C) on the dimol light emission at 703 nm (uncorrected for filter characteristics). Conditions: 37 °C, pH 7.4, in 80% D_2O phosphate buffer (50 mM).

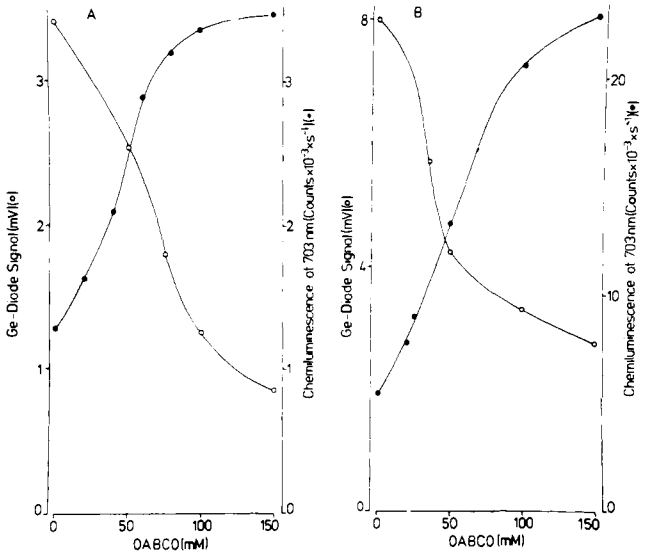

Figure 6. Dependence of monomol light emission (○) and dimol light emission (●) on DABCO concentration: (A) thermodissociation of $NDPO_2$ (7 mM), (B) hypochlorite/H_2O_2. $NDPO_2$ conditions are as described in the caption of Figure 5. At 37 °C, NaOCl (0.27 M) was infused at a rate of 20 μL min^{-1} during 5 min (total NaOCl infused was 9 mM) into 3 mL of 21 mM H_2O_2.

sition of the endoperoxide $NDPO_2$ was detected by the formation of $EASO_2$, the endoperoxide of EAS. Analysis of the HPLC chromatogram (Figure 1A) and UV spectrum (Figure 1B,C) of each of the products shows that the reaction is specific and that there is no other known contaminant species in the reaction mixture. In fact, EAS did not react with other oxidant species to produce $EASO_2$ (Table III). Hypochlorite, ozone, and hydroxyl radicals were reactive but did not yield $EASO_2$. Thus, the use of $NDPO_2$ as a singlet oxygen source and of EAS as a specific trap provides a useful method for the generation and detection of singlet oxygen. For comparison, $^1O_2$ was also generated by the reaction of hypochlorite/H_2O_2.

The capacity of EAS as a $^1O_2$ trap is measured by its β value, defined as the concentration of the probe at which 50% of the available $^1O_2$ is trapped. Botsivali and Evans[16] and Evans and Upton[17] reported the β value of EAS as 4.3×10^{-3} and 5.3×10^{-3} M, respectively. However, in Figure 2 the β value was found to be 7.7×10^{-3} M when $^1O_2$ was generated by $NDPO_2$ and $8 \times$

Table III. Reactivity of EAS with Oxidizing Species Monitored by HPLC[a]

system	product formed	
	$EASO_2$	other
EAS	–	–
EAS/$NDPO_2$	+	–
EAS/NaOCl	–	+
EAS/H_2O_2	–	–
EAS/H_2O_2/NaOCl	+	+
EAS/Fe^{2+}	–	–
EAS/H_2O_2/Fe^{2+}	–	+
EAS/xanthine/xanthine oxidase	–	–
EAS/ozone	–	+[b]
EAS/triplet oxygen	–	–

[a] Conditions: EAS (10 mM), $NDPO_2$ (5 mM), NaOCl (1.5 mM), H_2O_2 (2 mM), $FeSO_4$ (1.8 mM), xanthine (1 mM), xanthine oxidase (0.2 μM), triplet oxygen bubbling for 5 min. Incubation at 37 °C for 2 h in 50 mM phosphate buffer. HPLC conditions in Figure 1. [b] See ref 25.

10^{-3} M with the hypochlorite/H_2O_2 system, in agreement with data obtained by Schaap and co-workers ($\beta = 7.8 \times 10^{-3}$ M) using hypochlorite/H_2O_2.[20] $NDPO_2$ was employed in the present study as the $^1O_2$ source to avoid potential changes in the concentration of EAS due to the direct reaction of hypochlorite instead of $^1O_2$ (Table III). The $NDPO_2$ system has recently been used in biological studies.[26-28]

On the basis of the β value of EAS, the percentage of oxygen generated in the excited state by thermolysis of $NDPO_2$ was calculated to be 51%. Nieuwint and co-workers,[26] using a different $^1O_2$ trap, the potassium salt of rubrene-2,3,8,9-tetracarboxylic acid, reported the yield of $^1O_2$ from $NDPO_2$ as 48%. Thus, it appears that one-half of the O_2 liberated by thermolysis of $NDPO_2$ is in the singlet state. In contrast, the $^1O_2$ yield in the hypochlorite/H_2O_2 system is near unity, 87% as reported here and 86% at pH 7 reported with 2,5-dimethylfuran as trap.[29] The ability of the $NDPO_2$ system as a useful standard for light emission measurements was shown by the detection of the monomol and dimol

(26) Nieuwint, A. W. N.; Aubry, J. M.; Arwert, F.; Kortbeek, H.; Herzberg, S.; Joenje, H. *Free Radical Res. Commun.* **1985**, *1*, 1-9.
(27) Lafleur, M. V. M.; Nieuwint, A. W. M.; Aubry, J. M.; Kortbeek, H.; Arwert, F.; Joenje, H. *Free Radical Res. Commun.* **1987**, *2*, 343-350.
(28) Di Mascio, P.; Wefers, H.; Do-Thi, H. P.; Lafleur, M. V. M.; Sies, H. *Biochim. Biophys. Acta* **1989**, *1007*, 151-157.
(29) Held, A. M.; Halko, D. J.; Hurst, J. K. *J. Am. Chem. Soc.* **1978**, *100*, 5732-5739.

chemiluminescence correlated with $NDPO_2$ concentrations (Figure 3). It is important to note that the light emission by the $NDPO_2$ through the 634- and 703-nm filters is 53% of the total photoemission. Further $^1O_2$ characterization was performed by monitoring the effect of EAS and sodium azide in the monomol emission (Figure 4).

4.2. DABCO Effects. As mentioned above, an increase of $^1O_2$ dimol emission by DABCO has been described previously,[21,23,24] but the reason for this enhancement is unknown; it was suggested to be due to a change in the localized concentration of $^1O_2$ in solution or in the rate or extent of nucleation of oxygen bubbles.[23] The favoring of the emission due to a simultaneous transition involving a pair of $^1O_2$ molecules (dimol) should be accompanied by a decrease in the unimolecular decay (monomol). A decrease in monomol emission by DABCO has been described by Ogilby and Foote.[30] As can be seen in Figure 6, with $NDPO_2$ (Figure 6A) or hypochlorite/H_2O_2 (Figure 6B) as a source of $^1O_2$, the relationship between dimol and monomol emission is drastically affected by the presence of DABCO, as would be expected. A concentration of about 50 mM of DABCO is required to quench half of the singlet oxygen present in solution.[31] This value is similar to that which produces half of the loss of the monomol emission, as shown in Figure 6.

Kanofsky[32] reported that DABCO increases the rate of $^1O_2$ production in the reaction of H_2O_2 with OCl^- and attributed this catalysis as responsible for the enhancement of $^1O_2$ dimol emission described by Deneke and Krinsky.[21,23] As mentioned above, in our experiments DABCO had no effect on the yield in $EASO_2$ with $NDPO_2$ or hypochlorite/H_2O_2 as the $^1O_2$ source, and it did not change the decomposition kinetics of $NDPO_2$ (Figure 5A). DABCO increased the dimol signal (Figure 5C). DABCO has been described as being unreactive toward $^1O_2$ due to its effect in preventing or retarding the oxidation of known reactive acceptors of $^1O_2$.[33] Further studies on the reactivity of DABCO with $^1O_2$ using photooxidation with Rose bengal are in progress (Di Mascio, P.; Sies, H., in preparation).

4.3. Calibration of Monomol and Dimol Emission Using $^1O_2$ Yield of $NDPO_2$ Thermodissociation. The first derivative of the time course of $NDPO_2$ thermodissociation (Figure 5A) reveals a peak at 6 min at a rate of 75 μM NDP produced/min (not shown). This corresponds to an $^1O_2$ production rate of 38 μM/min, calculated with the $^1O_2$ yield of 50%. The signals in monomol and dimol emission (Figure 5B,C) give a calibration of 25 μM $^1O_2$ min^{-1} mV^{-1} in the monomol reaction and 38 μM $^1O_2$ min^{-1} $(200\ counts)^{-1}$ s^{-1} at 703 nm in the dimol reaction (uncorrected for filter characteristics). Expressed alternatively, 10 μM $^1O_2$/min corresponds to 0.4 mV in the germanium-diode signal (monomol) and to 14 counts s^{-1} in the 703-nm photoemission (dimol), taking into account the second power concentration dependence. This type of calibration can be carried out with different types of geometry and should be used for standardization.

Acknowledgment. We wish to thank Drs. Marisa H. G. Medeiros and Heribert Wefers for stimulating discussions. We also thanks Dr. H. Haddad, Department of Chemistry, Düsseldorf, for ^1H NMR and IR spectroscopy analysis. This work was supported by Deutsche Forschungsgemeinschaft, National Foundation for Cancer Research, and Fonds der Chemischen Industrie.

(30) Ogilby, P. R.; Foote, C. S. *J. Am. Chem. Soc.* **1983**, *105*, 3423-3430.
(31) Foote, C. S. In *Biochemical and Clinical Aspects of Oxygen*; Caughey, W. S., Ed.; Academic Press: New York, 1979; pp 613-625.
(32) Kanofsky, J. R. *Biochem. Biophys. Res. Commun.* **1986**, *134*, 777-782.
(33) Ouannes, C.; Wilson, T. *J. Am. Chem. Soc.* **1968**, *90*, 6527-6528.

The Correlation between Electronegativity Differences and Bond Energies

R. R. Reddy,* T. V. R. Rao, and R. Viswanath

Contribution from the Department of Physics, Sri Krishnadevaraya University, Anantapur 515 003, India. *Received February 2, 1988*

Abstract: A new formula relating electronegativity differences and bond energies is proposed. The relation has the form $D_{AB} = \bar{D}_{AB} + 32.058\Delta\chi$, where $\bar{D}_{AB} = (D_{AA}D_{BB})^{1/2}$ and $\Delta\chi$ represents the Pauling electronegativity difference. D_{AA} and D_{BB} are the bond energies of homonuclear molecules of the corresponding atoms of heteronuclear molecules. This relation is shown to yield accurate bond energies for both ionic and covalent bonds. A comparison with Pauling's formula $D_{AB} = \bar{D}_{AB} + 30\Delta\chi^2$ and Matcha's relation are also given. The bond energies estimated with the new formula agree within 3% of Match's bond energies. The corresponding error associated with Pauling's equation is about 45%. The proposed equation is found to be superior to the Pauling equation. This study may also be helpful in constructing the electronegativity scale.

I. Introduction

The bond dissociation energy of diatomic molecules is of fundamental importance in the studies of thermochemistry and astrophysics.[1] Thermal, spectroscopic, and mass spectrometric are the most important experimental methods[2-5] used to evaluate bond energy values. Methods for estimating dissociation energies theoretically continue to be proposed by workers[6-12] anxious to improve on Pauling's well-known relation[13]

$$D_{AB} = \bar{D}_{AB} + 30\Delta\chi^2 \quad (1)$$

(1) Gaydon, A. G. *Dissociation Energies*; Chapman and Hall: London, 1968.
(2) Herzberg, G. *Molecular spectra and Molecular structure*; Van Nostrand: New York, 1955.
(3) LeRoy, Robert L.; Bernstein, Richard B. *J. Mol. Spectrosc.* **1971**, *37*, 109.
(4) Hildenbrand, D. L.; Murad, E. *J. Chem. Phys.* **1969**, *51*, 807.
(5) Litzow, M. R.; Spalading, T. R. *Mass spectrometry of Inorganic and Organometallic Compounds*; American Elsevier: New York, 1973.
(6) Steele, D.; Lipincott, E. R.; Vanderslice, J. T. *Rev. Mod. Phys.* **1962**, *34*, 239.
(7) Somayajulu, G. R. *J. Chem. Phys.* **1963**, *34*, 1449.
(8) Preuss, H. *Theor. Chim. Acta* **1964**, *2*, 362.
(9) Ramani, K.; Ghodgaonkar, A. M. *J. Chem. Educ.* **1981**, *58*, 609.
(10) Reddy, R. R.; Reddy, A. S. R.; Krishna Reddy, V. *Theor. Chim. Acta* **1985**, *67*, 187.
(11) Reddy, R. R.; Reddy, A. S. R.; Krishna Reddy, V. *Can. J. Chem.* **1985**, *63*, 3174.
(12) Reddy, R. R.; Rao, T. V. R.; Reddy, A. S. R. *Proc. Indian Natl. Sci. Acad.* **1987**, *53A*, 506.

0002-7863/89/1511-2914$01.50/0